

Article

Amine-Modified Small Pore Mesoporous Silica as Potential Adsorbent for Zn Removal from Plating Wastewater

Vanpaseuth Phouthavong¹, Jae-Hyeok Park², Tatsuo Nishihama¹, Shuhei Yoshida¹, Takeshi Hagio^{1,2}, Yuki Kamimoto^{2,3} and Ryoichi Ichino^{1,2,*}

¹ Department of Chemical Systems Engineering, Graduate School of Engineering, Nagoya University, Furo-cho, Chikusa-ku, Nagoya 464-8603, Japan

² Institute of Materials Innovation, Institutes for Innovation for Future Society, Nagoya University, Furo-cho, Chikusa-ku, Nagoya 464-8601, Japan

³ Department of Environmental Science, Faculty of Human Environment, University of Human Environments, Okazaki 444-3505, Japan

* Correspondence: ichino.ryoichi@material.nagoya-u.ac.jp; Tel.: +81-52-747-3352

Abstract: The removal of Zn from wastewater generated from the Zn-based electroplating manufacturing process is essential because the regulation limit of Zn concentration in wastewater is becoming stricter in Japan. However, achieving this through conventional methods is difficult, especially for small and medium enterprises in the plating industry. Therefore, a suitable Zn-removal method with a low cost but high performance and Zn selectivity is required. The application of adsorbents is one possible solution. Mesoporous silica (MS) is a well-known adsorbent with controllable pore size, high specific surface area (SSA), high acid resistance, and ease of surface modification. In this study, we modified the surfaces of MSs with different initial pore sizes by amino groups and investigated their Zn removal performances. The effect of pore size on amine modification using (3-aminopropyl)triethoxysilane and on adsorption performance in a single system was investigated along with Zn adsorption selectivity in the Zn–Ni binary system. Amine-modified MS prepared from MS with an initial pore size of 1.9 nm showed drastically lower performance compared to those prepared from MS with an initial pore size larger than 2.8 nm. Zn-selectivity in the Zn–Ni binary system, containing equal amounts of Zn and Ni, was found to reach a maximum of 21.6 when modifying MS with an initial pore size of 2.8 nm.

Keywords: Zn removal; mesoporous silica; amine-modification; pore size; adsorption selectivity



Citation: Phouthavong, V.; Park, J.-H.; Nishihama, T.; Yoshida, S.; Hagio, T.; Kamimoto, Y.; Ichino, R. Amine-Modified Small Pore Mesoporous Silica as Potential Adsorbent for Zn Removal from Plating Wastewater. *Coatings* **2022**, *12*, 1258. <https://doi.org/10.3390/coatings12091258>

Academic Editor: Ioannis Anastopoulos

Received: 30 June 2022

Accepted: 25 August 2022

Published: 28 August 2022

Publisher's Note: MDPI stays neutral with regard to jurisdictional claims in published maps and institutional affiliations.



Copyright: © 2022 by the authors. Licensee MDPI, Basel, Switzerland. This article is an open access article distributed under the terms and conditions of the Creative Commons Attribution (CC BY) license (<https://creativecommons.org/licenses/by/4.0/>).

1. Introduction

Nowadays, protective coatings with high corrosion resistance are essential to extend the lifetime of industrial products, especially for those exposed to severe environments. Zn-based platings are the most commonly used coatings to improve corrosion resistance of steel products and research has been carried out to improve their corrosion resistance [1]. One of the most widely applied methods to improve the corrosion resistance of Zn electroplating is to form alloys of Zn with iron-group elements, e.g., Fe and Ni [2,3], due to its considerably low cost. In particular, Zn–Ni platings exhibit advanced corrosion resistance approximately six times greater than that of pure Zn plating and around three times greater than that of Zn–Fe platings when subjected to salt spray tests [3,4]. Therefore, Zn–Ni platings are adopted in various industrial products, including aircraft and automotive parts [5], to resist the harsh environments to which they are exposed. The rapid development of these industries has resulted in the generation of a vast amount of wastewater containing Zn from plating industries [6].

The hydroxide method is the most commonly used method to treat wastewater containing heavy metal ions because it is simple and low-cost [7]. This method involves the precipitation of metal hydroxide by increasing the pH of the wastewater, making it possible

to separate heavy metals as solid precipitates from the liquid. However, this method requires a large amount of chemicals and generates a vast amount of sludge [8]. Moreover, Zn removal presents difficulties compared to other heavy metals through the hydroxide method because Zn hydroxide starts to redissolve at high pH values and because various complexing agents in the plating wastewater obstruct precipitation. Recently, regulations that limit the Zn concentration in wastewater have become stricter, from 5 mg/L to 2 mg/L in Japan [9]. This target value was difficult to achieve through conventional removal methods for small and medium enterprises in the plating industry, and thus the adoption of regulation to 2 mg/L-Zn has been postponed to 2024. Therefore, the development of a suitable removal method with low cost, small footprint, high removal performance, and high selectivity is an urgent issue.

Several techniques have been developed to overcome drawbacks of the conventional chemical precipitation, such as bioprecipitation [10] and electroprecipitation [11]. These techniques are reported to be a cleaner and lower-cost process with high removal efficiency. Another effective technique, granulation, was also adopted in the Zn removal system called the fluidized-bed homogeneous granulation process [12]. The very high metal removal efficiency, up to 99%, can be accomplished using ultrafiltration [13]. These techniques are promising alternative protocols for effective removal/recovery of Zn and other metal ions from industrial wastewater; however, their process is rather complicated. Adsorption using adsorbents is a promising method because it has been reported to have high efficiency, a simple operating design, low-cost implementation, and it enables the removal of substances even at extremely low concentrations [14–17]. Various adsorbents have been developed or improved for selective adsorption of heavy metal ions in wastewater, such as polymer/metallic composites [18], zeolites and silica-based materials [19–24], carbon nanotubes [25], and activated carbon that was used in lab-scale tests [26] or was effectively adopted in water treatment innovation, namely, in a passive in-situ treatment system [27]. In addition to the synthetic adsorbents, natural biomass [28] and agricultural wastes [29] were also used as biosorbents to adsorb metal ions. These adsorbents were effective for removing Zn; however, the pore sizes of these adsorbents have a wide distribution, although the porosity of adsorbents is one of the main factors determining the adsorption capacity of adsorbents [30,31], or too small to improve performance by pore surface modification. Mesoporous silica (MS) is considered an interesting candidate due to its controllable pore diameter, high specific surface area (SSA), high acid resistance, and ease of surface modification [32,33]. In addition, its production cost is reported to be decreased by ~200 times by replacing the silica source from organic silica, such as TEOS, to cheaper silicon sources, which makes MS suitable for industrial use [34]. So far, cheaper commercial inorganic silica [34], natural clay derived silica [35], and industrial/agricultural waste derived silica [36] have been found to be effective in decreasing the cost of MS. Although MS itself shows low adsorption performance due to an amorphous surface structure, its adsorption performance can be tuned by embedding functional groups on its surface. Surface modification of MS for heavy metal adsorption is mostly developed based on two major conventional routes: (i) grafting (functional groups are introduced by post-treatment to MS) [37–41], and (ii) co-condensation (functional groups are pre-introduced in the precursors of MS) [42–45]. The most widely used method is grafting silane coupling agents to anchor the functional groups on the MS that are selective to particular metal ions. Among various functional groups, the amino group has high affinity for Zn [46], and thus the Zn adsorption capacity and selectivity of MS are expected to improve even under the coexistence of Ni ions.

Meanwhile, few studies have reported the effect of pore size on surface modification and adsorption performance. The effect of the MS pore structure on metal ion adsorption has been considered in several previous reports. For example, Kim et al. [47] studied the effect of framework and pore character of mercapto-functionalized MS on the adsorption of metal ions and found that the framework types of MS greatly influenced the density of mercapto-groups and metal ion uptake. They reported that the mercapto concentration

was strongly dependent on the framework pore volume and weakly correlated with pore size and the surface area of the supports. Idris et al. [48] investigated the Cr(VI) adsorption performance of amino-functionalized mesoporous silica using different MSs (USG-41, MCM-41, and SBA-15) and found that when using MS with a broader pore size distribution (USG-41) it gave higher Cr(VI) adsorption capacity than when using the narrower range ones (SBA-15 and MCM-41). Yuan et al. [49] compared the adsorption capacity of magnetic amino-functionalized mesoporous silica microspheres with two different pore sizes (2.1 and 9.9 nm) towards adsorption of Pb(II), Cu(II), and Cd(II). They found that the maximum adsorption capacities of these metal ions were increased approximately 3-fold when the adsorbents with larger pore sizes were used. It was explained that more amino groups were grafted onto the adsorbents when the pore size was larger. Knight et al. [50] found that MS with a smaller pore size resulted in improved Cu(II) adsorption performance and a pseudo-first order reaction rate constant. Although surface modified MSs have been intensively studied, the effect of pore size on surface modification and adsorption performance of Zn, especially in multi-cation systems, has not been clarified.

In this study, surface modification of MS with various pore sizes was carried out by using (3-aminopropyl)triethoxysilane (APTES) to study the effect of initial MS pore size on surface modification and Zn adsorption performance. In addition, the effect of the initial pore size of MS against Zn adsorption selectivity on amine-modified MS in Zn–Ni binary systems was investigated as a model for Zn–Ni plating wastewater.

2. Materials and Methods

2.1. Materials

Pristine MSs with five different pore sizes supplied from Taiyo Kagaku Co., Ltd., Yokkaichi, Japan (TMPS-1.5, TMPS-2.7, TMPS-4R, pore size: 1.9, 2.8, 3.9 nm) and Mitsubishi Chemical Co., Ltd., Tokyo, Japan (Mesopure[®], pore size: 5, 9 nm) were used in this experiment. A silane coupling agent, APTES (Sigma-Aldrich, Nacalai Special Grade Guaranteed Reagent, Nacalai Tesque, Inc., Kyoto, Japan), was used to modify the surface of the pristine MSs by amino-groups. Zinc sulfate heptahydrate ($\text{ZnSO}_4 \cdot 7\text{H}_2\text{O}$, JIS Special Grade Guaranteed Reagent, Nacalai Tesque, Inc., Kyoto, Japan) and nickel sulfate hexahydrate ($\text{NiSO}_4 \cdot 6\text{H}_2\text{O}$, JIS Special Grade Guaranteed Reagent, Nacalai Tesque, Inc., Kyoto, Japan) were used as the sources of Zn ions and Ni ions, respectively, and sulfuric acid (H_2SO_4 , JIS Special Grade Guaranteed Reagent, Nacalai Tesque, Inc., Kyoto, Japan) was used to adjust pH in the adsorption experiment, and H_2SO_4 and hydrochloric acid (HCl, JIS Special Grade Guaranteed Reagent, Nacalai Tesque, Inc., Kyoto, Japan) were used in the desorption experiment.

2.2. Surface Modification of MS

As-received MS samples were dried in an oven (DKN-402, Yamato Scientific Co., Ltd., Tokyo, Japan) at 110 °C for more than 24 h before surface modification. A total of 0.5 g of MSs were suspended in 50 mL of deionized water stored in a 100 mL glass vial, and 0.5 mL of silane coupling agent was added dropwise into this suspension. This suspension was sealed and shaken for 24 h at 25 °C. Then, the residual solid was collected and rinsed by suction filtration, followed by drying at 110 °C for 24 h. Scanning electron microscopy (SEM, JSM-6330F, JEOL, Tokyo, Japan) observations were carried out to confirm morphological changes before and after the treatment. The SSA and pore volume before and after the treatment were determined from the nitrogen adsorption at −196 °C using a gas sorption analyzer (Autosorb-1, Quantachrome Instruments, Boynton Beach, FL, USA). Hereafter, the MS modified by this method will be called amine-modified MS. The amount of modifying agent attached to the MS surface after 24 h of modification treatment was confirmed via a combustion method by using a carbon–sulfur simultaneous analysis device (EMIA-510, HORIBA Ltd., Kyoto, Japan). The samples were burned at 1350 °C in an oxygen atmosphere, and the carbon content in the generated gas was measured via infrared

absorption. The amount of modifying agent was calculated based on the expected carbon content of the modifying group.

2.3. Adsorption Experiment

Zn solution, Ni solution, and Zn–Ni binary solutions were prepared by dissolving sulfate salts, $\text{ZnSO}_4 \cdot 7\text{H}_2\text{O}$ or /and $\text{NiSO}_4 \cdot 6\text{H}_2\text{O}$, in deionized water prepared inhouse. Typically, distilled water was added up to 250 mL in a volumetric flask containing 0.112 g of $\text{ZnSO}_4 \cdot 7\text{H}_2\text{O}$ (1.5 mmol/L) or /and 0.098 g $\text{NiSO}_4 \cdot 6\text{H}_2\text{O}$ (1.5 mmol/L) and H_2SO_4 was added when pH adjustment was necessary; 50.0 mg of surface-modified MS was suspended in 50.0 mL of this solution and it was subsequently shaken for 24 h. The surface-modified MS was collected from the solution by filtration. Most experiments were carried out in the aforementioned conditions, but exceptions are the following experiments. Metal ion concentrations were varied in adsorption isotherm experiments (0.15–2.5 mmol/L–Zn) and adsorption in Zn–Ni binary systems (Zn/Ni = 1.5/1.5 and 0.2/1.5 mmol/L). In adsorption kinetic experiments, 100 mg of surface-modified MS was suspended in 100 mL of 1.5 mmol/L Zn solution, and 3 mL of the solution was extracted several times during shaking between 10–1440 min. The adsorption experiment conditions were basically repeated 2–5 times to ensure their reproducibility, except for those carried out in series, including isotherm, kinetics, and pH experiments.

The adsorption amount was calculated from the difference in initial and residual concentrations of metal ions in the solution determined by inductively coupled plasma atomic emission spectroscopy (ICP-AES, S-II, Seiko Instrument, Japan). The amount of adsorbed Zn^{2+} and Ni^{2+} (Q_{Zn} and Q_{Ni}) was calculated via the following equation:

$$Q_{\text{Me}} = ((C_0 - C_1) \times V) / m \quad (\text{Me} = \text{Zn or Ni})$$

Here, Q (mmol/g), C_0 (mmol/L), C_1 (mmol/L), V (L), and m (g) indicate the amount of adsorbed ion on the surface-modified MS, the initial and residual concentrations of Zn^{2+} or Ni^{2+} in the solution, the volume of the solution, and the mass of surface-modified MS used, respectively. Zn selectivity in the Zn–Ni binary system was calculated by dividing Q_{Zn} obtained in the Zn–Ni binary system by Q_{Ni} obtained in Zn–Ni binary system. X-ray photoelectron spectroscopy (XPS, ESCALAB 250Xi, Thermo Fisher Scientific, Waltham, MA, USA) equipped with an Al- $k\alpha$ (1486 eV) source was used to analyze the element valence on the surface of samples before and after the binary adsorption experiment to consider the adsorption mechanism. Individual high-resolution scans for N 1s, Ni 2p, and Zn 2p were taken at pass energy of 20 eV and 50 ms dwell time.

2.4. Desorption Experiment

The desorption of Zn adsorbed on each amine-modified MS was tested using 1 mol/L HCl and 0.5 mol/L H_2SO_4 solutions. A total of 30.0 mg of Zn adsorbed surface-modified MS was suspended in 30.0 mL of the acid solutions and it was subsequently shaken. The desorbed amount of Zn was analyzed using ICP-AES (S-II, Seiko instruments, Inc., Chiba, Japan) after 4 and 24 h and its recovered percentage of Zn was calculated as follows.

$$\%R = (C_{\text{des}} \times V_{\text{des}}) / (Q_{\text{Zn}} \times m_{\text{des}}) \times 100$$

Here, C_{des} (mmol/L), V_{des} (L), and m_{des} (g) indicate the concentrations of Zn^{2+} released into the acid solution, the volume of the acid solution, and the mass of surface-modified MS used in the desorption experiment, respectively.

3. Results and Discussion

3.1. The Effect of Pore Size of Mesoporous Silica on Surface Modification

Figure 1 shows the SEM images of MS before and after modification. No significant difference was observed in surface morphology regardless of the pore size of MSs. This

implies that the modification process did not destroy the structure of MS and also that no byproducts generated by the dehydration condensation reaction of excess APTES remain.

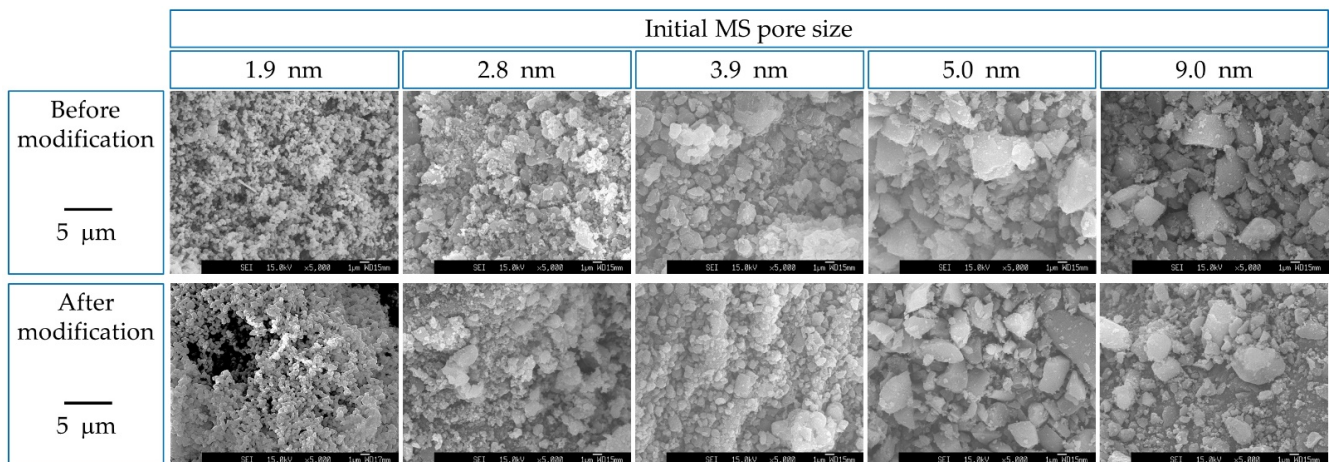


Figure 1. SEM image of MS before and after surface modification.

Figure 2 shows the amount of modifying agent embedded on each MS estimated from the carbon content of the amine-modified MSs. Only a small amount of modifying agent could be embedded on MS with a small pore size of 1.9 nm, while those with pore sizes between 2.8 and 9.0 nm were well embedded with modifying agents. Yuan et al. [49] reported a similar phenomenon when comparing the amount of amino-group grafted by using (3-aminopropyl)trimethoxysilane (APTMS) on MS magnetic microspheres with pore sizes of 2.2 and 10.3 nm. The amount of amino-group grafted onto the small pore sample was less than one-third of the amount grafted onto the large pore sample. The reason for the small amount of modifying agent embedded on MS with an initial pore size of 1.9 nm is probably because the pore was too small for the modifying agent to enter. The anticipated reason for the difference in the embedded amount of modifying agent will be discussed afterwards.

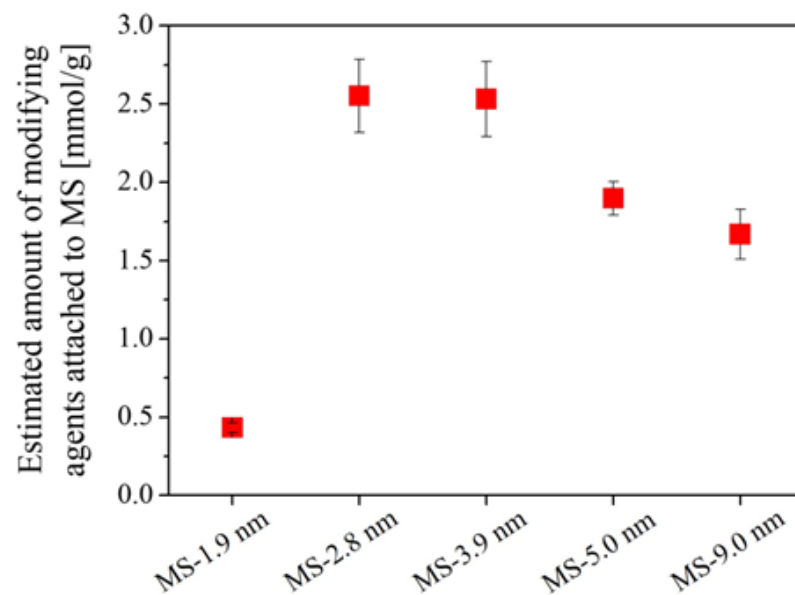


Figure 2. Amount of modifying agent embedded on MS with different pore sizes. Error bars indicate the standard deviation ($\pm\sigma$).

Figure 3 shows the SSA and pore volume of each MS before and after the surface modification with APTES. The SSA and pore volume decreased after modification in all

samples. In particular, a large decrease was observed for MSs with initial pore sizes of 1.9 and 2.8 nm. The reason for the large decrease for MS with an initial pore size of 2.8 nm can be explained by the large amount of modifying agent embedded in the MS pores, as shown in Figure 2; however, this is not the case for MS with an initial pore size of 1.9 nm. The amine-modified MS prepared from MS with an initial pore size of 1.9 nm had a drastically smaller SSA and pore volume even though only a small amount of modifying agent was embedded. This implies that modifying agents, namely APTES, could not effectively enter the pores when the initial MS pore was around 2 nm because the modifying agents embedded near the entrance of the MS pores must have clogged the pores of MS, hindering the modification of the inner walls of the MSs. The anticipated effect of the initial MS pore size against modification treatment is illustrated in Figure 4 along with the reaction of APTES on the MS surface. The especially small value of pore volume of the amine-modified MS prepared from MS with an initial pore size of 1.9 nm supports this hypothesis. MS with a pore size larger than 2.8 nm seemed to be essential for effective surface modification.

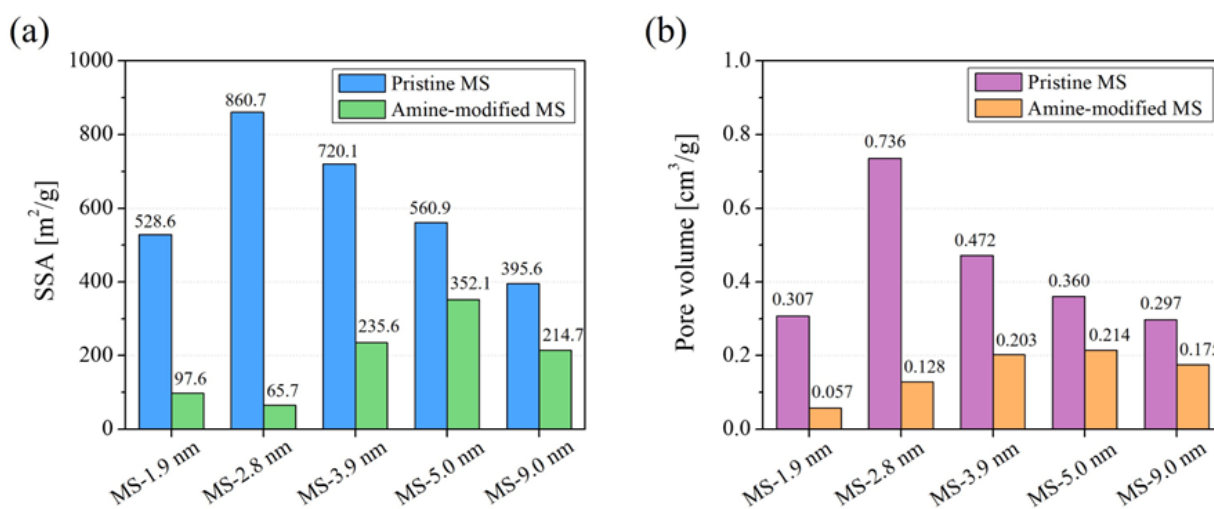


Figure 3. SSA (a) and pore volume (b) of MSs with different pore sizes before and after the surface modification.

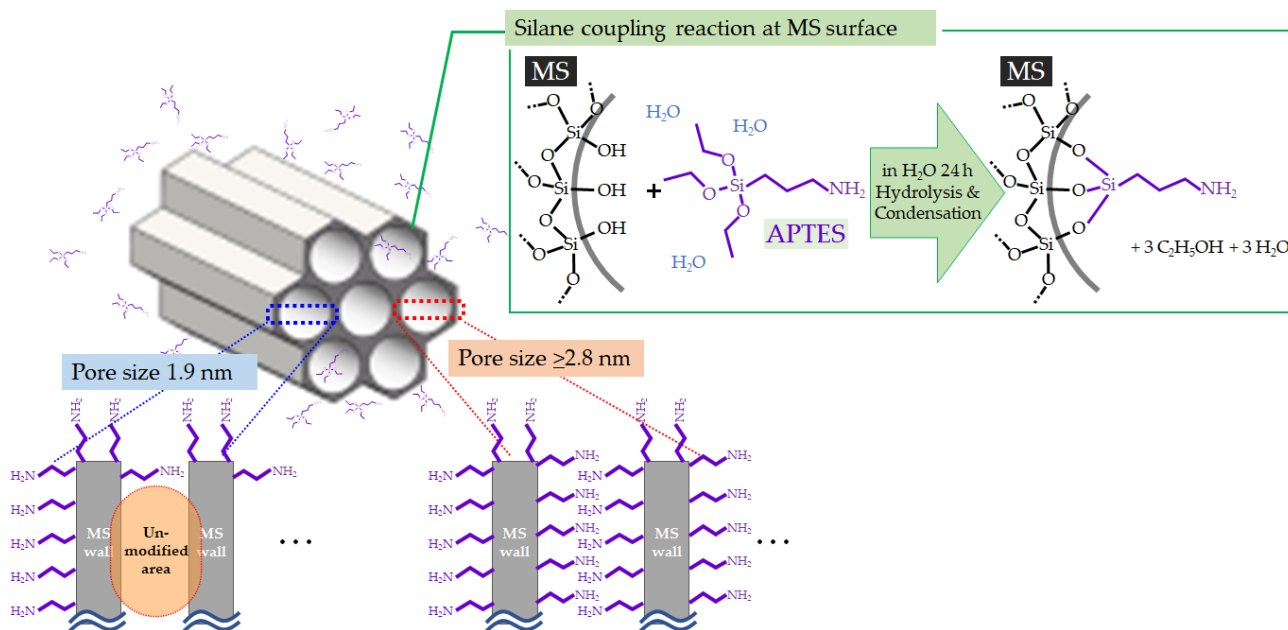


Figure 4. Expected reaction of APTES at the surface of MS and the anticipated effect of the difference in initial MS pore size.

3.2. Effect of Surface Modification of MS on Adsorption and Desorption Performance

Figure 5 shows the adsorption amount of Zn on surface-modified MS with different pore sizes in a Zn single-component system. Surface-modified MS with an initial pore size of 1.9 nm scarcely adsorbed Zn, unlike those with pores larger than 2.8 nm. The low Zn adsorption performance was anticipated due to the lesser amount of embedded modifying agent. This is supported by the fact that the SSA drastically decreased after modification by a factor of 5 compared to before modification, despite its low amount of embedded modifying agent. For the amine-modified MS prepared from MS with a pore size greater than 2.8 nm, the adsorption performance increased along with the decrease in pore size and saturated in the range of 2.8 to 3.9 nm. This may be related to the increase in SSA of the samples, considering that the silane coupling reaction takes place at the surface of the MSs. This also implies that the surface of MS with a pore size of more than 2.8 nm was effectively modified using APTES. The reason why the MS with the highest SSA before modification (MS-2.8 nm) did not show the highest adsorption performance may be due to the pore clogging inside the sample. The sample prepared from MS with an initial pore size of 2.8 nm showed the highest decrease in SSA and pore volume among all of the samples, even though the amount of modifying agent was nearly the same as that prepared from MS with an initial pore size of 3.9 nm. Therefore, the modifying agent may have clogged the pores and partially inhibited the modifying agents' access to the inner space in the MS.

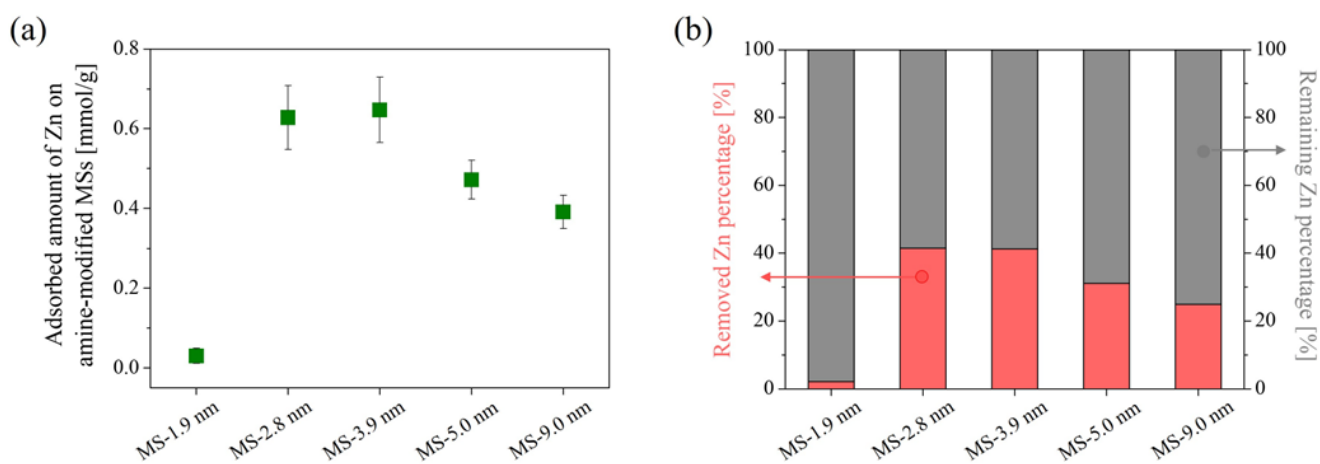


Figure 5. Zn adsorption amount on amine-modified MS with different initial MS pore sizes in single-component system (a) and their removed/remaining Zn percentage (b). Error bars indicate the standard deviation ($\pm\sigma$).

Statistical significance against Zn adsorption of each sample was validated by performing a one-way analysis of variance (ANOVA), followed by post hoc Bonferroni correction tests. The level of significance was set at $p \leq 0.05$ and $p \leq 0.005$ for the ANOVA and the post hoc tests, respectively. The results are shown in Table 1. The p value of ANOVA was significantly lower than 0.05, indicating there is a significant difference among the five amine-modified MSs. In addition, a significant difference was also detected between the samples prepared from MSs with small pores and large pores. This indicates that the initial pore size of MS obviously effects the performance of the prepared samples.

The relationship between the amount of modifying agent and the amount of Zn adsorbed is shown in Figure 6. The two parameters show good correlation, meaning that the adsorption of Zn in the Zn single-component system is mainly determined by the amount of modifying agent embedded on the MS surface. Because the slope is approximately one-fourth (indicated as a broken line in Figure 6), one Zn ion seems to be adsorbed to four amines. From this result, Zn adsorption on amine-modified MS seemed to be occurring by forming an amine-complex with four coordination. The Zn adsorption performance of amine-modified MSs with initial MS pore sizes of 9 nm was slightly lower than expected from the abovementioned relation, but this may be due to the embedment of oligomers in

the pores due to the large pore size of the initial MS. Because the Zn adsorption performance was low when using MS with an initial pore size of 1.9 nm, the results for amine-modified MSs with initial MS pore sizes of 1.9 nm are neglected hereafter.

Table 1. List of p values obtained in statistical tests.

Statistical Test	Samples Compared		p -Value
One-way ANOVA	All five samples		3.08×10^{-9} (<0.05)
Post hoc Bonferroni correction	Amine-modified MS-1.9	Amine-modified MS-2.8	6.14×10^{-5} (<0.005)
-	-	Amine-modified MS-3.9	1.69×10^{-5} (<0.005)
-	-	Amine-modified MS-5.0	2.73×10^{-5} (<0.005)
-	-	Amine-modified MS-9.0	8.94×10^{-6} (<0.005)
-	Amine-modified MS-2.8	Amine-modified MS-3.9	0.741 (>0.005)
-	-	Amine-modified MS-5.0	0.016 (>0.005)
-	-	Amine-modified MS-9.0	6.82×10^{-4} (<0.005)
-	Amine-modified MS-3.9	Amine-modified MS-5.0	0.008 (>0.005)
-	-	Amine-modified MS-9.0	2.60×10^{-4} (<0.005)
-	Amine-modified MS-5.0	Amine-modified MS-9.0	0.029 (>0.005)

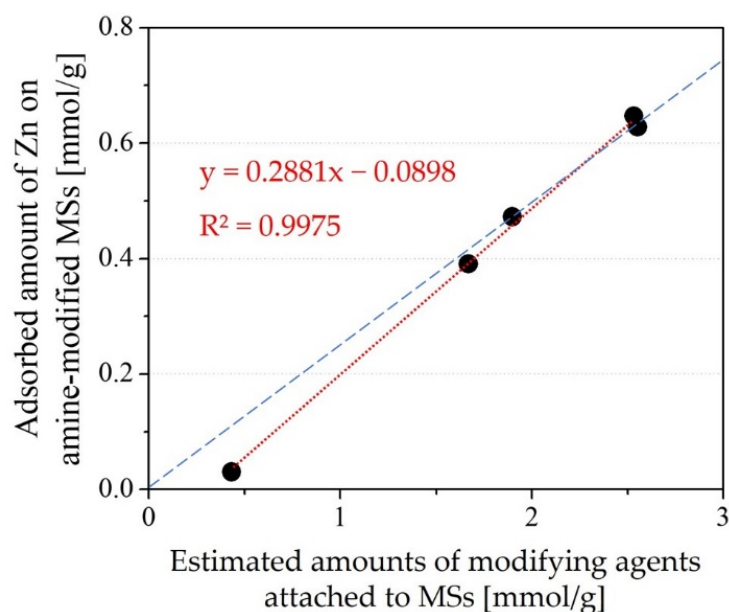


Figure 6. Relation between the amount of modifying agent and amount of Zn adsorbed in a single-component system. The broken line indicates $y = 0.25x$ (one Zn adsorbed against 4 amines).

The correlation coefficients against three isotherm models: Langmuir, Freundlich and Temkin and four kinetic models: Pseudo first-order, Pseudo second-order, Elovich, and Intraparticle diffusion, are shown in Table 2. As for isotherm models, Zn adsorption on the amine-modified MSs was found to fit well with the Langmuir isotherm model (>0.9) regardless of their initial pore size, as can be seen from the R^2 values in Table 2 and from the actual Langmuir plot shown in Figure 7. This indicates that Zn ions are attached to particular adsorption sites existing on amine-modified MSs, which well correlates with the assumption that amines of the surfaces of amine-modified MSs seem to be adsorbing Zn by forming an amine-complex, where amines serve as the adsorption sites. On the other hand, the result of the kinetic experiment proved that the pseudo-second-order model has the highest correlation coefficient (>0.999) among the considered models and well fitted all the adsorption kinetic process plots (Figure 8). This model is mainly based on the assumption that the react-limiting step is perhaps the chemisorption of sharing or exchanging electrons between the adsorbent and adsorbate [51,52], implying that the adsorption of Zn on amine-modified MSs is mainly chemisorption. The Elovich model, which describes chemical

adsorption mechanisms in nature [53], also showed a rather high correlation coefficient, further supporting that the adsorption is based on chemisorption. The adsorption kinetic also seems to make our assumption that the Zn amine-complex is formed explainable.

Table 2. Correlation coefficients against each isotherm models and kinetic models.

Samples	Isotherm Models				Kinetic Models		
	Langmuir	Freundlich	Temkin	Pseudo First-Order	Pseudo Second-Order	Elovich	Intraparticle Diffusion
Amine-modified MS-2.8 nm	$R^2 = 0.9654$	$R^2 = 0.1303$	$R^2 = 0.1279$	$R^2 = 0.9110$	$R^2 = 0.9997$	$R^2 = 0.9957$	$R^2 = 0.9208$
Amine-modified MS-3.9 nm	$R^2 = 0.9408$	$R^2 = 0.1717$	$R^2 = 0.1613$	$R^2 = 0.9307$	$R^2 = 0.9994$	$R^2 = 0.9949$	$R^2 = 0.9276$
Amine-modified MS-2.8 nm	$R^2 = 0.9818$	$R^2 = 0.0530$	$R^2 = 0.0500$	$R^2 = 0.9571$	$R^2 = 0.9995$	$R^2 = 0.9936$	$R^2 = 0.9308$
Amine-modified MS-2.8 nm	$R^2 = 0.9782$	$R^2 = 0.2099$	$R^2 = 0.1963$	$R^2 = 0.9193$	$R^2 = 0.9994$	$R^2 = 0.9947$	$R^2 = 0.9213$

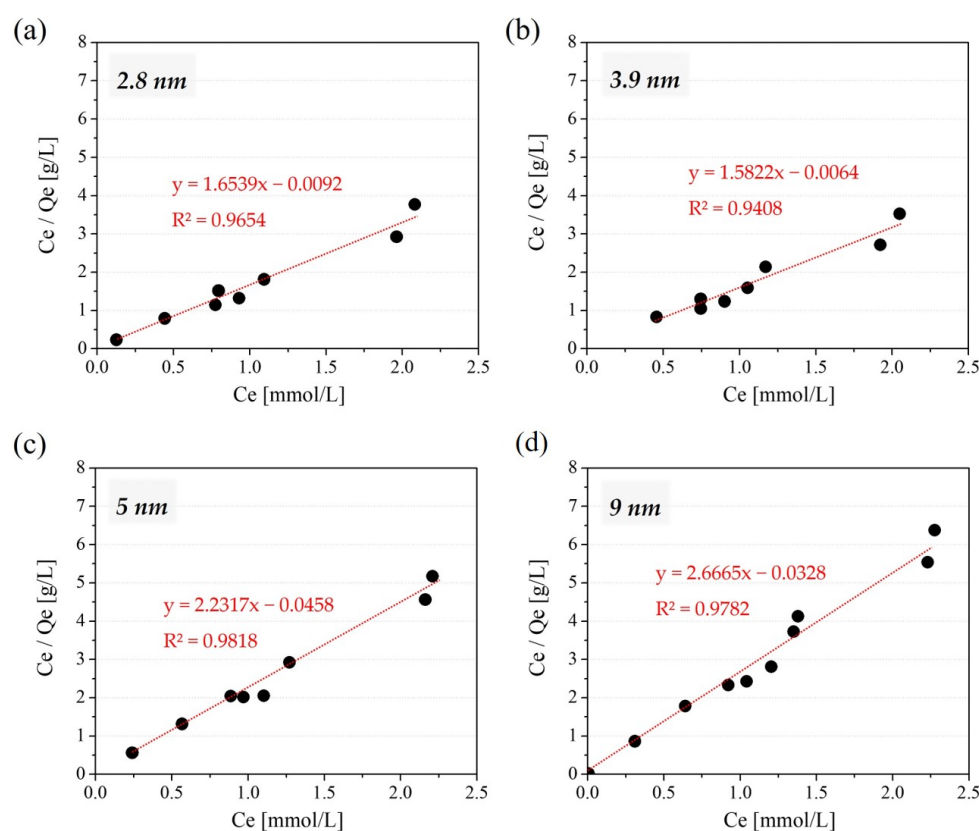


Figure 7. Langmuir plot for Zn adsorption amount on amine-modified MS with the initial MS pore size of 2.8 nm (a), 3.9 nm (b), 5 nm (c), and 9 nm (d) in a single-component system ranging from 0.15–2.5 mmol/L of Zn.

The Zn adsorption performances of the amine-modified MSs were compared with those of previously reported surface-modified MSs and other types of adsorbents (Table 3). The amine-modified MS with an initial pore size of 3.9 nm shows the highest Zn adsorption performance per gram, and that with an initial pore size of 2.8 nm showed the highest Zn adsorption performance per SSA in our work. The adsorbed amount of Zn per mass of adsorbent was higher than some MSs that were modified with amine [43,54–56] and other functional groups [39,57], and other types of adsorbents [18–24,26,29]; however, it was lower compared to some amine-modified MSs [37,38,58]. Meanwhile, when considering the adsorbed amount of Zn per SSA, our amine-modified MSs seemed to be superior compared to most adsorbents. This possibly means that the modified surface was accessible and well utilized for the adsorption of Zn. Thus, our material may be a promising adsorbent candidate for the removal of Zn from plating wastewater.

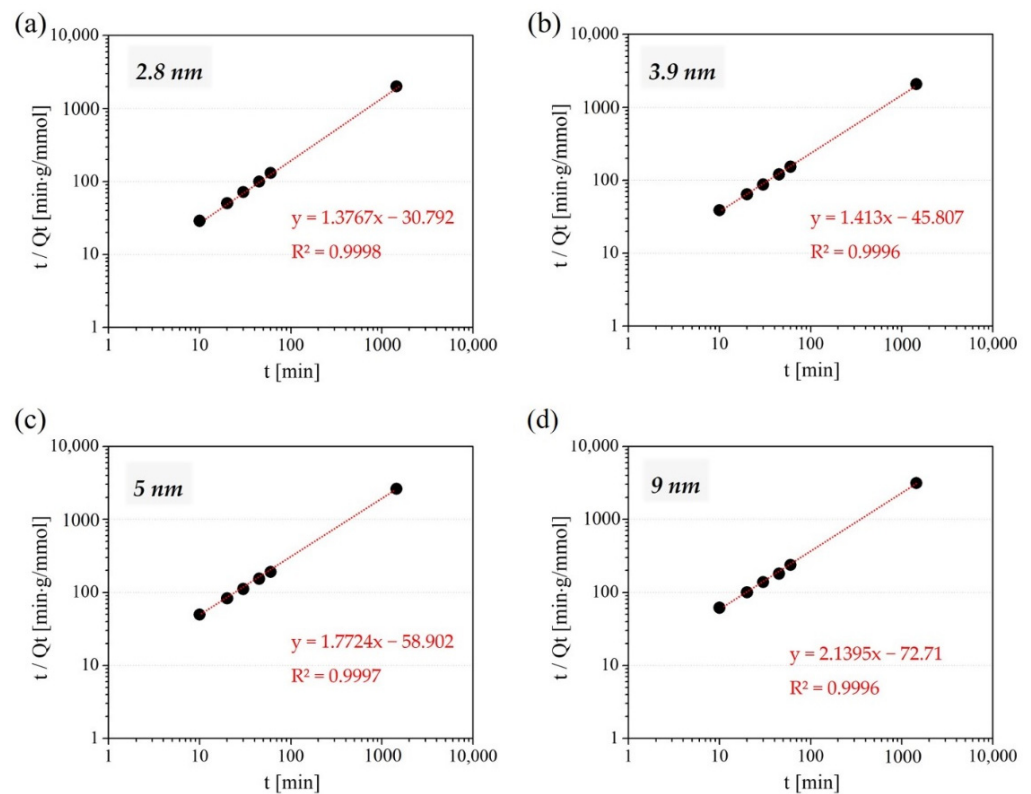


Figure 8. Pseudo second-order kinetic plot for Zn adsorption amount on amine-modified MS with the initial MS pore size of 2.8 nm (a), 3.9 nm (b), 5 nm (c), and 9 nm (d) in single-component system at various time intervals in the range of 10–1440 min.

Table 3. Comparison of Zn adsorption performance of the amine-modified MSs with other adsorbents.

Adsorbents	SSA (m ² /g)	Zn Adsorption Performance		References
		Adsorbed Amount per Mass of Adsorbent (mmol/g)	Adsorbed Amount per SSA of Adsorbent (μmol/m ²)	
<i>Surface modified mesoporous silica</i>				
Amine-modified MS-2.8 nm	65.7	0.605	9.208	This work
Amine-modified MS-3.9 nm	235.6	0.635	2.693	This work
Amine-modified MS-5.0 nm	352.1	0.448	1.273	This work
Amine-modified MS-9.0 nm	214.7	0.375	1.747	This work
Amine-functionalized magnetic core-MS shell	236	0.632	2.677	[54]
Amine-MCM-41	750	0.734	0.979	[38]
Sodium dodecyl sulfate-modified amine-MCM-41	285	0.088	0.310	[55]
Amine-SBA-15	345	2.251	6.531	[37]
Amine-SBA-15	293.94	0.784	2.668	[58]
Amine-SBA-15	373	0.208	0.558	[56]
Sheet amine-MCM	189.9	0.214	1.132	[43]
5-methyl-2-thiophenecarboxaldehyde-immobilized SBA-15	623	0.489	0.780	[39]
Platinum and propyl sulfonic acid-SBA-15	745.12	0.358	0.480	[57]
<i>Other adsorbents</i>				
NiO-MgO embedded-silica nanoparticles	48	0.576	12.083	[22]
Granular sludge-clay	24.53	0.019	0.766	[24]
FAU-type zeolite	432	0.562	1.302	[23]
Lanthanum-modified zeolite	55.7	0.367	6.577	[19]
Porous(styrene-divinylbenzen)/CuNi bimetallic nanocomposite microsphere	25.88	0.315	12.157	[18]
Cysteamine-montmorillonite nanocomposite	58.7	0.256	4.359	[20]
Magnetic zeolite/cellulose nanofiber nanocomposite	Not reported	0.145	-	[21]
Commercial activated carbon	1241	0.214	0.168	[26]
Coconut coir	16.7	0.023	1.401	[29]
Rice husk	8.1	0.014	1.682	[29]

Table 4 shows the results of a desorption experiment of Zn using 1.0 mol/L HCl and 0.5 mol/L H₂SO₄ solutions. The concentration of acid was adjusted to unify the number of protons in the system. Although there was a small difference according to the type of acid, the %R was slightly higher when using 1.0 mol/L HCl solution than 0.5 mol/L H₂SO₄ solution in all conditions. This indicates that HCl was more suitable for regeneration. Furthermore, no obvious increase in %R was found by extending the desorption time from 4 to 24 h, meaning that 4 h was enough for regeneration. Interestingly, amine-modified MSs with smaller initial pore sizes (2.8 and 3.9 nm) showed higher %R values than those with larger initial pores (5.0 and 9.0 nm). These results indicate that amine-modified MSs with smaller initial pore sizes are promising because they can adsorb and recover more Zn compared to those with larger initial pore sizes than 5.0 nm.

Table 4. Recovered percentage of Zn, %R, using acid solutions.

Samples	1.0 mol/L HCl Solution		0.5 mol/L H ₂ SO ₄ Solution	
	4 h	24 h	4 h	24 h
Amine-modified MS-2.8 nm	78%	78%	71%	71%
Amine-modified MS-3.9 nm	87%	87%	83%	81%
Amine-modified MS-5.0 nm	69%	69%	66%	63%
Amine-modified MS-9.0 nm	72%	70%	67%	67%

Figure 9 shows the adsorption amount of Ni on surface-modified MS with different pore sizes in a Ni single-component system. The results showed a similar trend and adsorption amount to those for Zn adsorption in the single-component system, although a slight increase in the adsorption amount was observed for pore sizes of 5.0 nm and 9.0 nm. This means that the pores were accessible to Ni ions as well as Zn ions, and no selectivity resulting from sieving by the size of ions was taking place. Moreover, considering that the adsorption amount of Ni was nearly equivalent to that of Zn, Ni adsorption on amine-modified MS may also be due to the formation of an amine-complex with four coordination.

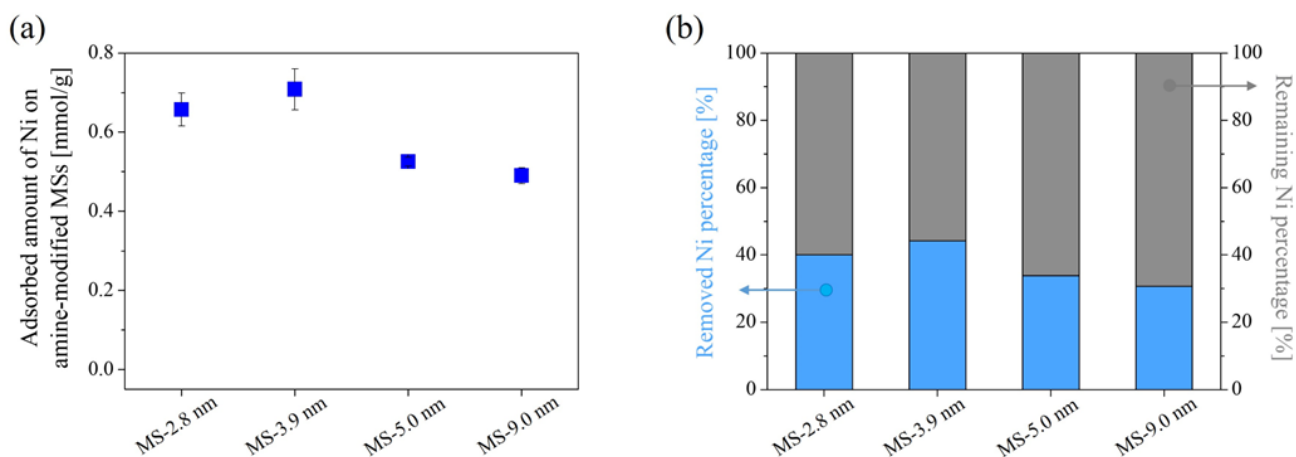


Figure 9. Ni adsorption amount on amine-modified MS with different initial MS pore sizes in a single-component system (a) and their removed/remaining Ni percentage (b). Error bars indicate the standard deviation ($\pm\sigma$).

3.3. Effect of Surface Modification of MS on Adsorption Selectivity

Figure 10 shows the adsorption amount of Zn and Ni in a Zn–Ni binary system as a model of Zn–Ni plating wastewater, and Figure 11 shows the Zn/Ni selectivity in binary systems containing 1.5 mmol/L of both Zn and Ni. The ratios of Q_{Zn} and Q_{Ni} obtained in a single-component adsorption experiment in the presence of only Zn or Ni (Q_{Zn} (in single-component system)/ Q_{Ni} (in single-component system)) are plotted together in Figure 11 to confirm whether the selectivity can be explained by the difference in adsorption amount

in the single-component system. When the Zn concentration in the solution was higher than the capacity, almost only Zn was adsorbed (Figure 10a), and when the Zn concentration in the solution was lower than the capacity, Zn was completely removed to below the detection limit of the ICP-AES (Figure 10b). These results imply that Zn is selectively removed from the solution regardless of the Ni concentration in the system. In the system with 1.5 mmol/L Zn or Ni (Figure 11), the results obtained for the single-component system barely show any selectivity (Q_{Zn} (in single-component system)/ Q_{Ni} (in single-component system) = 0.89 ± 0.1) and are similar regardless of the pore size. This means that both Zn and Ni are accessible to the adsorption sites when they exist individually, and no selectivity caused by sieving of ionic size is observed. Meanwhile, the results obtained for the binary system containing equimolar amounts of Zn and Ni (1.5 mmol/L) were significantly different. Although both Zn and Ni ions were able to adsorb on amine-modified MSs, most of the ions adsorbed on the amine-modified MS were Zn, as can be seen from Figure 10a. The Zn concentration drastically decreased while that of Ni barely changed after adsorption tests for all amine-modified MSs, meaning that the amine-modified MSs selectively adsorbed Zn regardless of the pore size of MS. This is probably attributed to the larger stability constant of the Zn amine complex ($\log\beta_4 = 9.46$) than the Ni amine complex ($\log\beta_4 = 7.04$) [59]. Meanwhile, Zn/Ni selectivity in the binary system was found to be the highest for amine-modified MS prepared from MS with a pore size of 2.8 nm. This may be because adsorbed Zn ions stabilized in the pore openings of amine-modified MSs, which limited the entrance of Ni ions, owing to less free space in the small pores. Another possibility is that the position and distance of the amines were more appropriate for Zn to form a stable complex. An illustration of this idea is shown in Figure 12. Again, the one-way ANOVA was conducted to confirm the difference in Zn/Ni selectivity. The p value of ANOVA was 0.037, which is lower than 0.05, indicating that there was a significant difference among the Zn/Ni selectivity within the four amine-modified MSs.

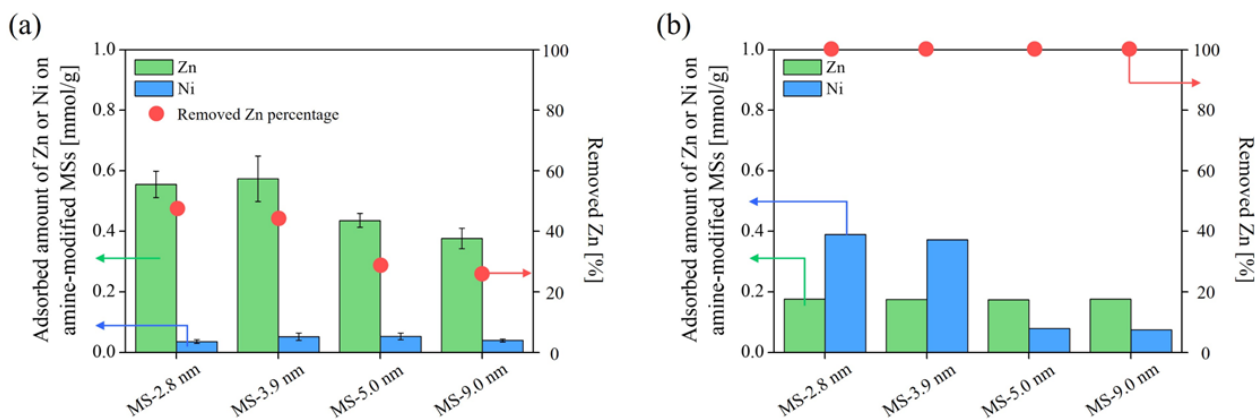


Figure 10. Adsorption amount of Zn and Ni on amine-modified MS with different initial MS pore sizes in Zn–Ni binary system. Concentration of each element is Zn/Ni = 1.5/1.5 mmol/L (a) and Zn/Ni = 0.2/1.5 mol/L (b).

Figure 13 shows the effect of pH on the adsorption amount of Zn and Ni in a Zn–Ni binary system using amine-modified MSs prepared from MSs with an initial pore size of 2.8 nm and 9 nm, as a representative of high and low Zn selective samples in this study. It is evident that the amine-modified MSs prepared from the small 2.8 nm pore MS maintained higher selectivity in both pH 4 to 6. Amine-modified MS is reported to be positively charged in this pH range [60], in contrast to pristine MSs, which are negatively charged [61]. Therefore, the electrostatic effect seems to not be the cause of this difference. Perhaps the competitive adsorption of protons on amine at a low pH may be the reason for this difference. The selection of the initial MS pore size seems to be effective to enhance the Zn selectivity of amine-modified MS at various pH values. In addition, it was found

that the pH should be higher than 4 for effective Zn adsorption, regardless of the initial MS pore size. This is important information to use in practical applications.

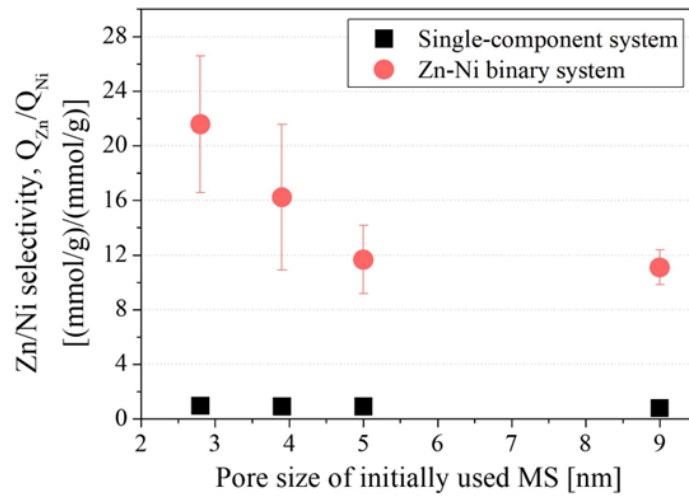


Figure 11. Zn/Ni selectivity of amine-modified MS with different initial MS pore sizes in single-component and binary systems (Zn = Ni = 1.5 mmol/L). Plots of the single-component system are ratios of Q_{Zn} and Q_{Ni} obtained in the previous single-component adsorption experiment in the presence of only Zn or Ni. Error bars indicate the standard deviation ($\pm\sigma$).

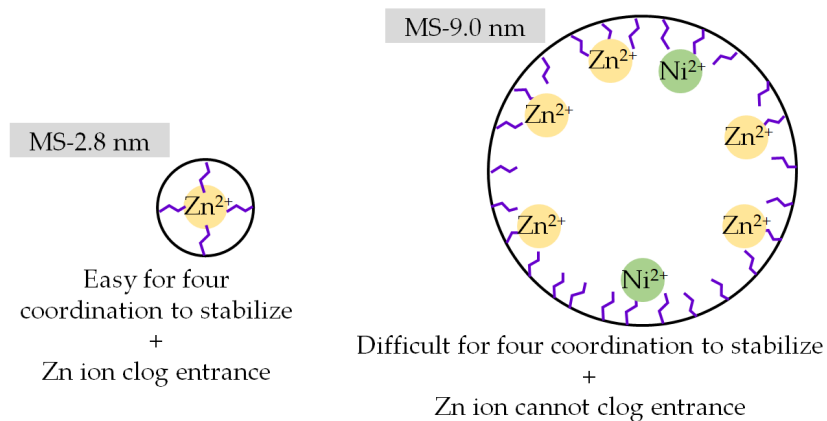


Figure 12. Illustration on anticipated adsorption of Zn and Ni on amine-modified MS with different initial MS pore sizes in binary systems.

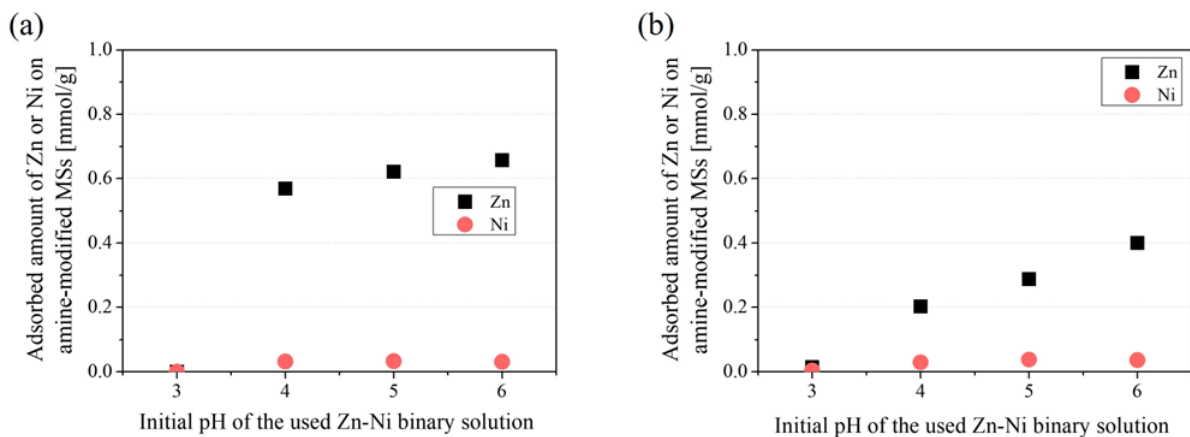


Figure 13. Effect of initial pH on adsorption amount of Zn and Ni on amine-modified MS prepared from MSs with initial pore sizes of 2.8 nm (a) and 9 nm (b) in the Zn-Ni binary system.

Finally, the adsorption mechanism was considered from the XPS analysis results on the surface of samples before and after the binary adsorption experiment. The XPS spectra of the amine-modified MS prepared from MSs with initial pore sizes of 2.8 nm and 9 nm in the Zn–Ni binary system are shown in Figure 14. The XPS survey spectra presented in Figure 14a shows that neither Zn nor Ni signals are detected, and nitrogen related to the amines embedded by surface modification is detected in pristine MSs. This explains the impartment of the amine group to the surface of MSs by amine treatment [62]. Meanwhile, Zn is clearly confirmed while Ni is scarcely seen even in high-resolution spectra after the Zn–Ni binary adsorption experiment (Figure 14b,c). This correlates well with the result that Ni was barely adsorbed onto amine-modified MSs. Meanwhile, the high-resolution Zn 2p spectra in Figure 14b present a bond between Zn ion and nitrogen ($\text{Zn}^{2+}\text{-N}$) that is formed after adsorption. Moreover, when comparing the intensity of $\text{Zn}^{2+}\text{-N}$ bonding, it can be seen that the peak of $\text{Zn}^{2+}\text{-N}$ is more intense for amine-modified MS prepared from MS with initial pore sizes of 2.8 nm than that of 9.0 nm. Related to this change, peaks of -NH_2 observed in high-resolution N 1s spectra in Figure 14d decrease, implying that the number of free NH_2 decreases due to bonding with Zn^{2+} . This implies that a more stable bond is formed when using MS with a smaller initial pore size. This result is in accordance with the expectation proposed in Figure 12 that amine-complexes are more difficult to form in large pores due to the limitations of positions of amine around the Zn and Ni ions. Furthermore, no peaks of bonding between Ni ions and nitrogen are observed from the XPS spectra from Ni, implying the very small amount of the Ni amine complex formation. This can be explained by the lower stability constant of the Ni-amine complex than the Zn-amine complex, as discussed beforehand.

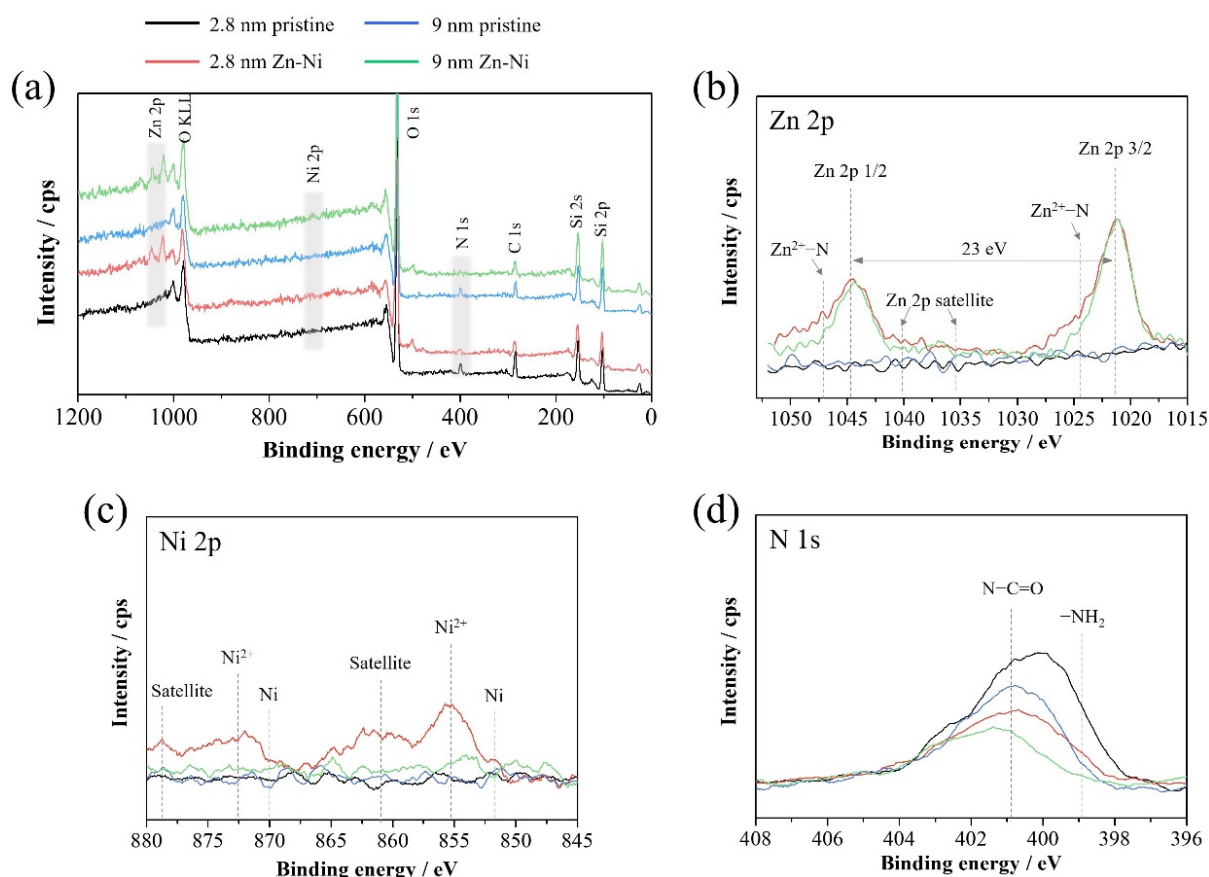


Figure 14. XPS survey spectra of the amine-modified MS prepared from MSs with initial pore sizes of 2.8 nm and 9 nm (a), and core-level spectra for Zn 2p (b), Ni 2p (c), and N 1s (d) in the Zn–Ni binary system.

4. Conclusions

Modification of MS using APTES was investigated for removing Zn from Zn–Ni plating wastewater. When the initial pore size of MS was 1.9 nm, MS could be barely modified and showed low adsorption performance. Clogging of the pores by surface-modifying groups appeared to be the cause of this low performance. Meanwhile, MS with a pore size larger than 2.8 nm was well modified and showed high Zn-adsorption performance. All amine-modified MS samples were found to exhibit Zn-selective adsorption in the Zn–Ni binary system, while they did not show selective adsorption in the single-component systems. The larger stability constant of the Zn amine complex than the Ni amine complex was apparently the cause of this selective adsorption. Moreover, Zn/Ni selectivity in the binary system was found to be the highest for surface-modified MS prepared from MS with a pore size of 2.8 nm. The amine-modified MS prepared from MS with a pore size of 2.8 nm appears to be a promising adsorbent for treating wastewater generated from Zn–Ni plating processes with both high adsorption amount and Zn selectivity.

Author Contributions: Conceptualization, Y.K.; methodology, S.Y. and T.N.; validation, S.Y. and T.N.; formal analysis, V.P., J.-H.P. and T.H.; investigation, S.Y. and T.N.; resources, R.I.; data curation, T.H.; writing—original draft preparation, V.P. and T.H.; writing—review and editing, J.-H.P.; visualization, V.P. and T.H.; supervision, R.I.; project administration, Y.K.; funding acquisition, R.I. All authors have read and agreed to the published version of the manuscript.

Funding: This research was partially funded by Japan Science and Technology Agency, Japan, the Strategic International Collaborative Research Program (SICORP) (JPMJSC18H1) and the Ministry of Education, Culture, Sports, Science and Technology, Japan, Project of Creation of Life Innovation Materials for Interdisciplinary and International Researcher Development.

Institutional Review Board Statement: Not applicable.

Informed Consent Statement: Not applicable.

Data Availability Statement: Data is contained within the article.

Acknowledgments: The authors appreciate the partial support from the Strategic International Collaborative Research Program (SICORP) (JPMJSC18H1) from the Japan Science and Technology Agency, Japan and Project of Creation of Life Innovation Materials for Interdisciplinary and International Researcher Development of the Ministry of Education, Culture, Sports, Science and Technology, Japan. In addition, we express our gratitude to Hideki Hayashi, Nagoya Municipal Industrial Research Institute, for assistance in BET measurements.

Conflicts of Interest: The authors declare no conflict of interest.

References

1. Park, J.-H.; Hagio, T.; Kamimoto, Y.; Ichino, R.; Lee, M.-H. Enhancement of corrosion resistance by lamination of Mg film on Zn-55Al-1.6Si-coated steel by physical vapor deposition. *Surf. Coat. Technol.* **2020**, *387*, 125537. [CrossRef]
2. Yadav, A.; Katayama, H.; Noda, K.; Masuda, H.; Nishikata, A.; Tsuru, T. Effect of Fe–Zn alloy layer on the corrosion resistance of galvanized steel in chloride containing environments. *Corros. Sci.* **2007**, *49*, 3716–3731. [CrossRef]
3. Shibuya, A.; Kurimoto, T.; Korekawa, K.; Noji, K. Corrosion-resistance of Electroplated Ni-Zn Alloy Steel Sheet. *Tetsu-to-Hagane* **1980**, *66*, 771–778. [CrossRef]
4. Qun, Z.L. Electrodeposition of zinc-iron alloy from an alkaline zincate bath. *Met. Finish.* **1998**, *96*, 54–57. [CrossRef]
5. Gnanamuthu, R.; Mohan, S.; Saravanan, G.; Lee, C.W. Comparative study on structure, corrosion and hardness of Zn–Ni alloy deposition on AISI 347 steel aircraft material. *J. Alloys Compd.* **2012**, *513*, 449–454. [CrossRef]
6. Fu, F.; Wang, Q. Removal of heavy metal ions from wastewaters: A review. *J. Environ. Manag.* **2011**, *92*, 407–418. [CrossRef]
7. John, M.; Heuss-Aßbichler, S.; Ullrich, A. Recovery of Zn from wastewater of zinc plating industry by precipitation of doped ZnO nanoparticles. *Int. J. Environ. Sci. Technol.* **2016**, *13*, 2127–2134. [CrossRef]
8. Kongsricharoern, N.; Polprasert, C. Electrochemical precipitation of chromium (Cr⁶⁺) from an electroplating wastewater. *Water Sci. Technol.* **1995**, *31*, 109–117. [CrossRef]
9. Website of Ministry of the Environment, Government of Japan. Available online: <http://www.env.go.jp/press/109976.html> (accessed on 25 June 2022). (In Japanese)
10. Kumar, M.; Pakshirajan, K. Continuous removal and recovery of metals from wastewater using inverse fluidized bed sulfidogenic bioreactor. *J. Clean. Prod.* **2020**, *284*, 124769. [CrossRef]

11. Lim, S.S.; Fontmorin, J.-M.; Pham, H.T.; Milner, E.; Abdul, P.M.; Scott, K.; Head, I.; Yu, E.H. Zinc removal and recovery from industrial wastewater with a microbial fuel cell: Experimental investigation and theoretical prediction. *Sci. Total Environ.* **2021**, *776*, 145934. [[CrossRef](#)]
12. Udomkitthawewat, N.; Anotai, J.; Choi, A.E.; Lu, M.C. Removal of zinc based on a screw manufacturing plant wastewater by fluidized-bed homogeneous granulation process. *J. Clean. Prod.* **2019**, *230*, 1276–1286. [[CrossRef](#)]
13. Innocenzi, V.; Prisciandaro, M.; Tortora, F.; di Celso, G.M.; Vegliò, F. Treatment of WEEE industrial wastewaters: Removal of yttrium and zinc by means of micellar enhanced ultra filtration. *Waste Manag.* **2018**, *74*, 393–403. [[CrossRef](#)] [[PubMed](#)]
14. Sophia, A.C.; Lima, E.C. Removal of emerging contaminants from the environment by adsorption. *Ecotoxicol. Environ. Saf.* **2018**, *150*, 1–17. [[CrossRef](#)]
15. Siyal, A.A.; Shamsuddin, M.R.; Low, A.; Rabat, N.E. A review on recent developments in the adsorption of surfactants from wastewater. *J. Environ. Manag.* **2019**, *254*, 109797. [[CrossRef](#)]
16. Rath, B.S.; Kumar, P.S. Application of adsorption process for effective removal of emerging contaminants from water and wastewater. *Environ. Pollut.* **2021**, *280*, 116995. [[CrossRef](#)] [[PubMed](#)]
17. Gupta, V.K.; Carrott, P.J.M.; Carrott, M.M.L.R. Suhas Low-Cost Adsorbents: Growing Approach to Wastewater Treatment—a Review. *Crit. Rev. Environ. Sci. Technol.* **2009**, *39*, 783–842. [[CrossRef](#)]
18. Hridya, T.; Varghese, E.; Harikumar, P. Removal of heavy metals from aqueous solution using porous (Styrene-divinylbenzene)/CuNi bimetallic nanocomposite microspheres. *Environ. Nanotechnol. Monit. Manag.* **2021**, *16*, 100606. [[CrossRef](#)]
19. Wang, Z.; Li, W.; Zhu, J.; Wang, D.; Meng, H.; Wang, H.; Li, J. Simultaneous adsorption of phosphate and zinc by lanthanum modified zeolite. *Environ. Technol. Innov.* **2021**, *24*, 101906. [[CrossRef](#)]
20. Wang, G.; Xiao, H.; Zhu, J.; Zhao, H.; Liu, K.; Ma, S.; Zhang, S.; Komarneni, S. Simultaneous removal of Zn²⁺ and p-nitrophenol from wastewater using nanocomposites of montmorillonite with alkyl-ammonium and complexant. *Environ. Res.* **2021**, *201*, 111496. [[CrossRef](#)]
21. Mirjavadi, E.S.; Tehrani, R.M.A.; Khadir, A. Effective adsorption of zinc on magnetic nanocomposite of Fe₃O₄/zeolite/cellulose nanofibers: Kinetic, equilibrium, and thermodynamic study. *Environ. Sci. Pollut. Res.* **2019**, *26*, 33478–33493. [[CrossRef](#)]
22. Abuhatab, S.; El-Qanni, A.; Al-Qalaq, H.; Hmoudah, M.; Al-Zerei, W. Effective adsorptive removal of Zn²⁺, Cu²⁺, and Cr³⁺ heavy metals from aqueous solutions using silica-based embedded with NiO and MgO nanoparticles. *J. Environ. Manag.* **2020**, *268*, 110713. [[CrossRef](#)] [[PubMed](#)]
23. Joseph, I.V.; Tosheva, L.; Doyle, A.M. Simultaneous removal of Cd(II), Co(II), Cu(II), Pb(II), and Zn(II) ions from aqueous solutions via adsorption on FAU-type zeolites prepared from coal fly ash. *J. Environ. Chem. Eng.* **2020**, *8*, 103895. [[CrossRef](#)]
24. Du, X.; Cui, S.; Fang, X.; Wang, Q.; Liu, G. Adsorption of Cd(II), Cu(II), and Zn(II) by granules prepared using sludge from a drinking water purification plant. *J. Environ. Chem. Eng.* **2020**, *8*, 104530. [[CrossRef](#)]
25. Chen, Z.; Fu, D.; Koh, K.Y.; Chen, J.P. A new carbon nanotube modified by nano CaO₂ for removal of chromate and phosphate from aqueous solutions. *Chem. Eng. J.* **2022**, *446*. [[CrossRef](#)]
26. Shahrokhi-Shahraki, R.; Benally, C.; El-Din, M.G.; Park, J. High efficiency removal of heavy metals using tire-derived activated carbon vs commercial activated carbon: Insights into the adsorption mechanisms. *Chemosphere* **2020**, *264*, 128455. [[CrossRef](#)]
27. Bortone, I.; Santonastaso, G.; Erto, A.; Chianese, S.; Di Nardo, A.; Musmarra, D. An innovative in-situ DRAINage system for advanced groundwater reactive TREATment (in-DRAIN-TREAT). *Chemosphere* **2020**, *270*, 129412. [[CrossRef](#)]
28. Lekshmi, R.; Rejiniemon, T.S.; Sathya, R.; Kuppusamy, P.; Al-Mekhlafi, F.A.; Wadaan, M.A.; Rajendran, P. Adsorption of heavy metals from the aqueous solution using activated biomass from *Ulva flexuosa*. *Chemosphere* **2022**, *306*, 135479. [[CrossRef](#)]
29. Tokay, B.; Akpınar, I. A comparative study of heavy metals removal using agricultural waste biosorbents. *Bioresour. Technol. Rep.* **2021**, *15*, 100719. [[CrossRef](#)]
30. Li, B.; Gan, L.; Owens, G.; Chen, Z. New nano-biomaterials for the removal of malachite green from aqueous solution via a response surface methodology. *Water Res.* **2018**, *146*, 55–66. [[CrossRef](#)]
31. Andreas, A.; Winata, Z.G.; Santoso, S.P.; Angkawijaya, A.E.; Yuliana, M.; Soetaredjo, F.E.; Ismadji, S.; Hsu, H.-Y.; Go, A.W.; Ju, Y.-H. Biocomposite hydrogel beads from glutaraldehyde-crosslinked phytochemicals in alginate for effective removal of methylene blue. *J. Mol. Liq.* **2021**, *329*, 115579. [[CrossRef](#)]
32. Zhang, F.; Yang, H. Multifunctional mesoporous silica-supported palladium nanoparticles for selective phenol hydrogenation in the aqueous phase. *Catal. Sci. Technol.* **2014**, *5*, 572–577. [[CrossRef](#)]
33. Li, Z.; Barnes, J.C.; Bosoy, A.; Stoddart, J.F.; Zink, J.I. Mesoporous silica nanoparticles in biomedical applications. *Chem. Soc. Rev.* **2012**, *41*, 2590–2605. [[CrossRef](#)] [[PubMed](#)]
34. Kittappa, S.; Cui, M.; Ramalingam, M.; Ibrahim, S.; Khim, J.; Yoon, Y.; Snyder, S.A.; Jang, M. Synthesis Mechanism and Thermal Optimization of an Economical Mesoporous Material Using Silica: Implications for the Effective Removal or Delivery of Ibuprofen. *PLoS ONE* **2015**, *10*, e0130253. [[CrossRef](#)]
35. Yu, Z.-H.; Zhai, S.-R.; Guo, H.; Lv, T.-M.; Song, Y.; Zhang, F.; Ma, H.-C. Removal of methylene blue over low-cost mesoporous silica nanoparticles prepared with naturally occurring diatomite. *J. Sol-Gel Sci. Technol.* **2018**, *88*, 541–550. [[CrossRef](#)]
36. Razak, N.A.A.; Othman, N.H.; Shayuti, M.S.M.; Jumahat, A.; Sapiai, N.; Lau, W.J. Agricultural and industrial waste-derived mesoporous silica nanoparticles: A review on chemical synthesis route. *J. Environ. Chem. Eng.* **2022**, *10*, 107322. [[CrossRef](#)]
37. Giraldo, L.; Moreno-Pirajan, J.C. Study on the adsorption of heavy metal ions from aqueous solution on modified SBA-15. *Mater. Res.* **2013**, *16*, 745–754. [[CrossRef](#)]

38. Chen, X.; Ching, W.K.; Lam, K.F.; Wei, W.; Yeung, K.L. An Investigation of the Selective Adsorptions of Metals on Mesoporous NH₂-MCM-41. *J. Phys. Chem. C* **2016**, *120*, 18365–18376. [[CrossRef](#)]
39. Parambadath, S.; Mathew, A.; Barnabas, M.J.; Kim, S.Y.; Ha, C.-S. Concentration-dependant selective removal of Cr(III), Pb(II) and Zn(II) from aqueous mixtures using 5-methyl-2-thiophenecarboxaldehyde Schiff base-immobilised SBA-15. *J. Sol-Gel Sci. Technol.* **2015**, *79*, 426–439. [[CrossRef](#)]
40. Taba, P.; Hala, Y.; Budi, P.; Wiyanto, E.; Pratiwi, M.D. Amine-functionalized MCM-48 as adsorbent of Zn²⁺ and Ni²⁺ ions. *Int. J. Eng. Res. Appl.* **2018**, *5*, 107–116.
41. Alswieleh, A.M.; Albahar, H.Y.; Alfawaz, A.M.; Alsilme, A.S.; Beagan, A.M.; Alsahme, A.M.; Almeataq, M.S.; Alshahrani, A.; Alotaibi, K.M. Evaluation of the Adsorption Efficiency of Glycine-, Iminodiacetic Acid -, and Amino Propyl-Functionalized Silica Nanoparticles for the Removal of Potentially Toxic Elements from Contaminated Water Solution. *J. Nanomater.* **2021**, *2021*, 6664252. [[CrossRef](#)]
42. Han, Y.; Fang, K.; Gu, X.; Chen, J.; Chen, J. Amino-Functionalized Mesoporous Silicas MCM-48 as Zn(II) Sorbents in Water Samples. *J. Chem. Eng. Data* **2012**, *57*, 2059–2066. [[CrossRef](#)]
43. Nakanishi, K.; Tomita, M.; Kato, K. Synthesis of amino-functionalized mesoporous silica sheets and their application for metal ion capture. *J. Asian Ceram. Soc.* **2015**, *3*, 70–76. [[CrossRef](#)]
44. Yang, H.; Hu, Y.; Wang, X.; Fu, W.; Tian, H.; Alam, E. Investigation on synthesis of ion-imprinted mesoporous adsorbents by using ultrasound- and microwave-assisted preparation and their dynamic adsorption properties on heavy metals. *Environ. Sci. Pollut. Res.* **2019**, *26*, 10987–10999. [[CrossRef](#)] [[PubMed](#)]
45. Wieszczycka, K.; Filipowiak, K.; Wojciechowska, I.; Buchwald, T.; Siwińska-Ciesielczyk, K.; Strzemiecka, B.; Jesionowski, T.; Voelkel, A. Novel highly efficient ionic liquid-functionalized silica for toxic metals removal. *Sep. Purif. Technol.* **2021**, *265*, 118483. [[CrossRef](#)]
46. Zhang, L.; Zhang, J.; Jiang, Q.; Zhang, L.; Song, W. Zinc binding groups for histone deacetylase inhibitors. *J. Enzym. Inhib. Med. Chem.* **2018**, *33*, 714–721. [[CrossRef](#)]
47. Kim, Y.; Lee, B.; Yi, J. Effect of Framework and Textural Porosities of Functionalized Mesoporous Silica on Metal Ion Adsorption Capacities. *Sep. Sci. Technol.* **2005**, *39*, 1427–1442. [[CrossRef](#)]
48. Idris, S.A.; Alotaibi, K.M.; Peshkur, T.A.; Anderson, P.; Morris, M.; Gibson, L.T. Adsorption kinetic study: Effect of adsorbent pore size distribution on the rate of Cr (VI) uptake. *Microporous Mesoporous Mater.* **2012**, *165*, 99–105. [[CrossRef](#)]
49. Yuan, Q.; Li, N.; Chi, Y.; Geng, W.; Yan, W.; Zhao, Y.; Li, X.; Dong, B. Effect of large pore size of multifunctional mesoporous microsphere on removal of heavy metal ions. *J. Hazard. Mater.* **2013**, *254–255*, 157–165. [[CrossRef](#)]
50. Knight, A.; Tigges, A.B.; Ilgen, A.G. Adsorption of copper (II) on mesoporous silica: The effect of nano-scale confinement. *Geochem. Trans.* **2018**, *19*, 13. [[CrossRef](#)]
51. Ambe, S. Adsorption kinetics of antimony(V) ions onto α -ferric oxide surfaces from an aqueous solution. *Langmuir* **1987**, *3*, 489–493. [[CrossRef](#)]
52. Zhang, H.; Li, L.; Zhou, S. Kinetic modeling of antimony(V) adsorption–desorption and transport in soils. *Chemosphere* **2014**, *111*, 434–440. [[CrossRef](#)] [[PubMed](#)]
53. Wu, F.-C.; Tseng, R.-L.; Juang, R.-S. Characteristics of Elovich equation used for the analysis of adsorption kinetics in dye-chitosan systems. *Chem. Eng. J.* **2009**, *150*, 366–373. [[CrossRef](#)]
54. Alam, E.; Feng, Q.; Yang, H.; Fan, J.; Mumtaz, S. Synthesis of magnetic core-shell amino adsorbent by using uniform design and response surface analysis (RSM) and its application for the removal of Cu²⁺, Zn²⁺, and Pb²⁺. *Environ. Sci. Pollut. Res.* **2021**, *28*, 36399–36414. [[CrossRef](#)]
55. Kaewprachum, W.; Wongsakulphasatch, S.; Kiatkittipong, W.; Striolo, A.; Cheng, C.K.; Assabumrungrat, S. SDS modified mesoporous silica MCM-41 for the adsorption of Cu²⁺, Cd²⁺, Zn²⁺ from aqueous systems. *J. Environ. Chem. Eng.* **2020**, *8*, 102920. [[CrossRef](#)]
56. Lachowicz, J.I.; Delpiano, G.R.; Zanda, D.; Piludu, M.; Sanjust, E.; Monduzzi, M.; Salis, A. Adsorption of Cu²⁺ and Zn²⁺ on SBA-15 mesoporous silica functionalized with triethylenetetramine chelating agent. *J. Environ. Chem. Eng.* **2019**, *7*, 103205. [[CrossRef](#)]
57. Çitak, A. Synthesis, characterization, and kinetic studies of multifunctionalized mesoporous silica for adsorption of zinc. *Turk. J. Chem.* **2019**, *43*, 106–117. [[CrossRef](#)]
58. Wu, W.; Guo, W.; Ji, Z.; Liu, Y.; Hu, X.; Liu, Z. Static and dynamic sorption study of heavy metal ions on amino-functionalized SBA-15. *J. Dispers. Sci. Technol.* **2017**, *39*, 594–604. [[CrossRef](#)]
59. Kondo, K.; Nakagawa, S.-I.; Matsumoto, M.; Yamashita, T.; Furukawa, I. Selective Adsorption of Metal Ions on Novel Chitosan-Supported Sulfonic Acid Resin. *J. Chem. Eng. Jpn.* **1997**, *30*, 846–851. [[CrossRef](#)]
60. Chang, J.-H.; Mou, K.Y.; Mou, C.-Y. Sleeping Beauty Transposon-Mediated Asparaginase Gene Delivery by a Nanoparticle Platform. *Sci. Rep.* **2019**, *9*, 11457. [[CrossRef](#)]
61. Liu, M.; Hou, L.-A.; Yu, S.; Xi, B.; Zhao, Y.; Xia, X. MCM-41 impregnated with A zeolite precursor: Synthesis, characterization and tetracycline antibiotics removal from aqueous solution. *Chem. Eng. J.* **2013**, *223*, 678–687. [[CrossRef](#)]
62. Soyekwo, F.; Zhang, Q.; Gao, R.; Qu, Y.; Lv, R.; Chen, M.; Zhu, A.; Liu, Q. Metal in situ surface functionalization of polymer-grafted-carbon nanotube composite membranes for fast efficient nanofiltration. *J. Mater. Chem. A* **2016**, *5*, 583–592. [[CrossRef](#)]